Electronic Supplementary Information

Enhancing phase separation with conformation-locked nonfullerene acceptor for over 14.4% efficiency organic solar cells

Zhuohan Zhang,[a] Xin Liu,[b] Jiangsheng Yu,[,b] Hongtao Wang,[a] Ming Zhang,[c] Linqiang Yang,[a] Renyong Geng,[a] Jinru Cao,[a] Fuqiang Du,[a] Feng Liu,*[,c] and Weihua Tang*[,a]*

[a]Key Laboratory of Soft Chemistry and Functional Materials, Ministry of Education, Nanjing University of Science and Technology, Nanjing 210094, China.
[b]MIIT Key Laboratory of Advanced Solid Laser, Nanjing University of Science and Technology, Nanjing 210094, P. R. China.
[c]Department of Physics and Astronomy, and Collaborative Innovation Center of IFSA (CICIFSA), Shanghai Jiaotong University, Shanghai 200240, China

Table of Content

1. Materials and Synthesis

All commercially available chemicals and solvents were purchased from Aladdin, Sigma-Aldrich, or J&K Chemical Co., and used without further purification. 2-(5,6-difluoro-3-oxo-2,3-dihydro-1H-inden-1-ylidene) malononitrile were purchased from Derthon Optoelectronic Materials Science Technology Co. LTD.. Non-fullerene IT-4F was purchased from SunaTech Inc., while polymer donor PM7 was purchased from Solarmer Materials Inc.. ITC6-CHO and ITC6-IC was synthesized on the basis of our previous work [1]. Anhydrous THF and toluene were freshly distilled over sodium wire/benzophenone prior to use, and 1,2-dichloroethane was dried with calcium hydride. The detailed synthetic processes of ITC6-4F are described in the following.

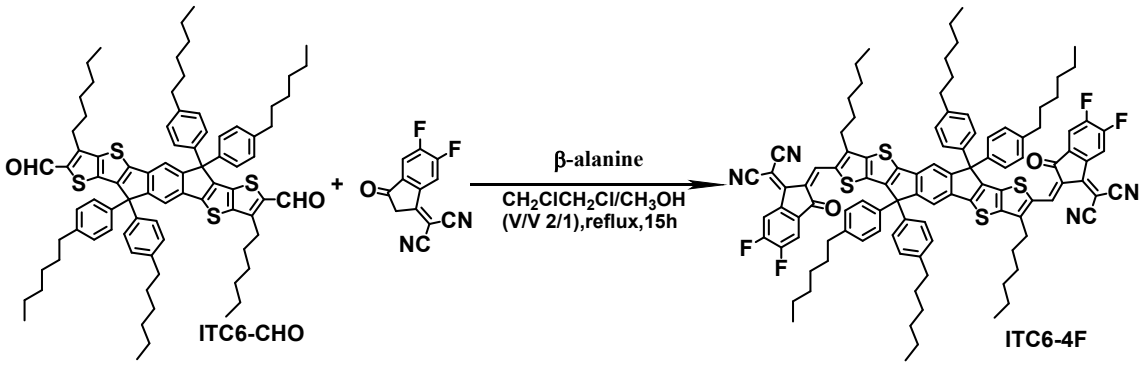

Scheme S1 Synthetic route of ITC6-4F.

Synthesis of 2,2'-[[3,9-dihexyl-6,6,12,12-tetrakis(4-hexylphenyl)-6,12-dihydrodithieno[2,3-*d*:2',3'-*d'*]-s-indaceno[1,2-*b*:5,6-*b'*]dithiophene-2,8-diyl]bis[methylidyne(5,6-difluoro-3-oxo-1H-indene-2,1(3H)-diylidene)]]bispropanedinitrile (ITC6-4F)

ITC6-CHO (120.00 mg, 96.47 μmol) and β-alanine (1.72mg, 19.29 μmol) were dissolved in $ClCH_2CH_2Cl/CH_3OH$ (6 ml/3 ml). 2-(5,6-difluoro-3-oxo-2,3-dihydro-1H-inden-1-ylidene)malononitrile (222.05 mg, 0.96 mmol) was then added and the mixture stirred and refluxed for 15 hours. The resulting mixture was extracted with chloroform, washed with water, and dried over $MgSO_4$. After removal the solvent, the crude product was purified on a silica-gel column chromatography to afford 115 mg of compound **ITC6-4F** in 75.3% yield as a purple solid. ^1H NMR (500 MHz, $CDCl_3$ δ): 9.03 (s, 2H),

8.54 (dd, J = 9.9, 6.4 Hz, 2H), 7.66 (s, 2H), 7.64 (s, 2H), 7.24 -7.17 (m, 8H), 7.14 (d, J = 8.2 Hz, 8H), 3.12 (t, J = 7.9 Hz, 4H), 2.56 (dd, J = 8.9, 6.8 Hz, 8H), 1.75 (q, J = 7.8 Hz, 4H), 1.59 (dd, J = 11.1, 4.8 Hz, 8H), 1.46 (d, J = 8.8 Hz, 4H), 1.33 (dq, J = 7.3, 5.3, 3.3 Hz, 16H), 1.27 (td, J = 7.0, 3.5 Hz, 16H), 0.91- 0.82 (m, 18H). ^{13}C NMR (125 MHz, $CDCl_3$ δ): 186.17, 159.26, 156.03, 155.66, 155.56, 153.51, 153.00, 148.20, 145.80, 145.77, 142.82, 139.14, 137.21, 136.77, 135.81, 135.05, 134.70, 129.11, 128.11, 120.41, 118.92, 115.24, 115.16, 115.07, 114.81, 112.82, 112.68, 68.92, 63.60, 35.86, 31.95, 31.82, 31.52, 31.41, 30.08, 29.96, 29.68, 29.44, 22.84, 22.74, 14.34, 1.28, 0.25. ^{19}F NMR (470 MHz, $CDCl_3$ δ): -122.18 (dt, J = 17.4, 8.4 Hz), -123.36 (dt, J = 15.6, 7.5 Hz). HRMS (ESI) *m/z*: $[M + H]^+$ calcd for $C_{106}H_{102}F_4N_4O_2S_4$, 1666.6822; found, 1666.6805.

2. Instruments and general methods

The ^{1}H NMR, ^{13}C NMR spectra were measured using Bruker AVANCE 500 MHz spectrometer. Mass spectra were measured using GCT-MS EI and Bruker Daltonics Biflex III MALDI-TOF Analyzer in the MALDI mode. Ultraviolet - visible (UV-Vis) absorption spectra were recorded on a UV-Vis instrument Evolution 220 (Thermo Fisher). The electrochemical cyclic voltammetry (CV) was conducted on an electrochemical workstation (CHI760E Chenhua Shanghai) with Pt plate as working electrode, Pt slice as counter electrode, and Ag/AgCl electrode as reference electrode in tetrabutylammonium hexafluorophosphate (Bu_4NPF_6, 0.1 M) acetonitrile solutions at a scan rate of 50 mV s^{-1}. Ferrocene/ferrocenium (Fc/Fc^+) was used as the internal standard (the energy level of Fc/Fc^+ is -4.8 eV under vacuum), and the formal potential of Fc/Fc^+ was measured as 0.35 V vs. Ag/AgCl electrode. Thermogravimetric analysis (TGA) was conducted under nitrogen atmosphere at a heating rate of 20 °C min^{-1} from 50 °C to 800 ℃. The instrument type was TGA/SDTA851E (Mettler Toledo).

3. NMR, Mass Spectra, and TGA

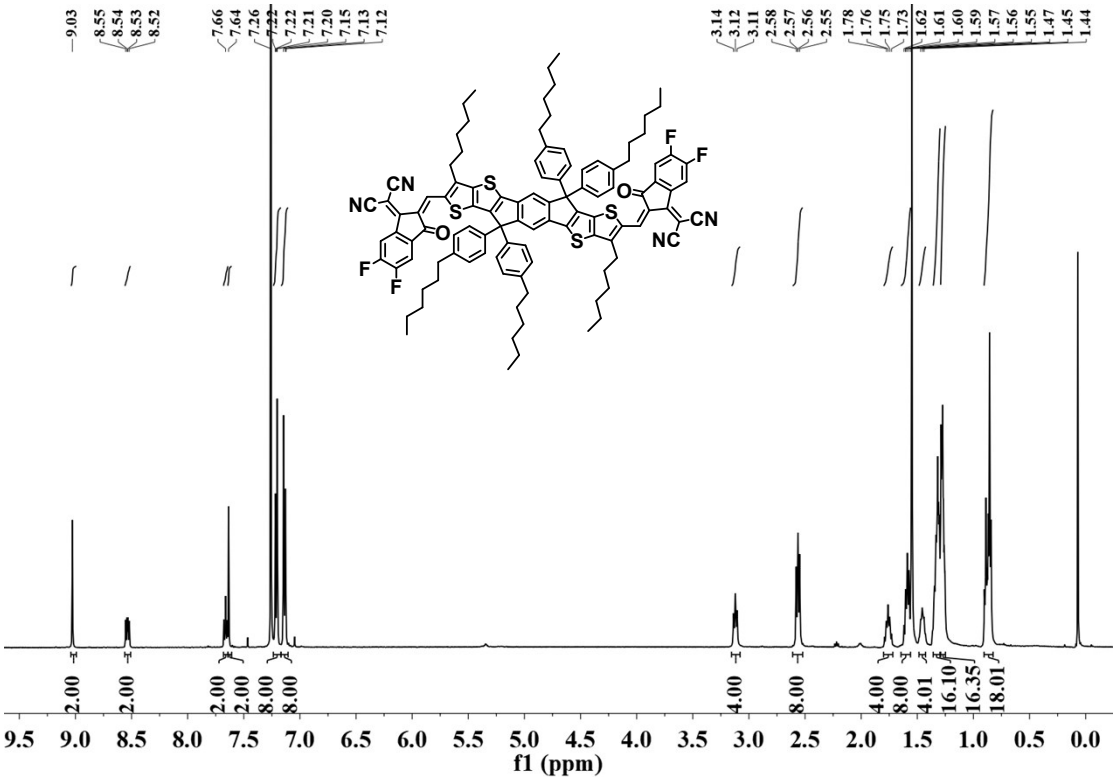

Fig. S1 ^{1}H NMR of **ITC6-4F**.

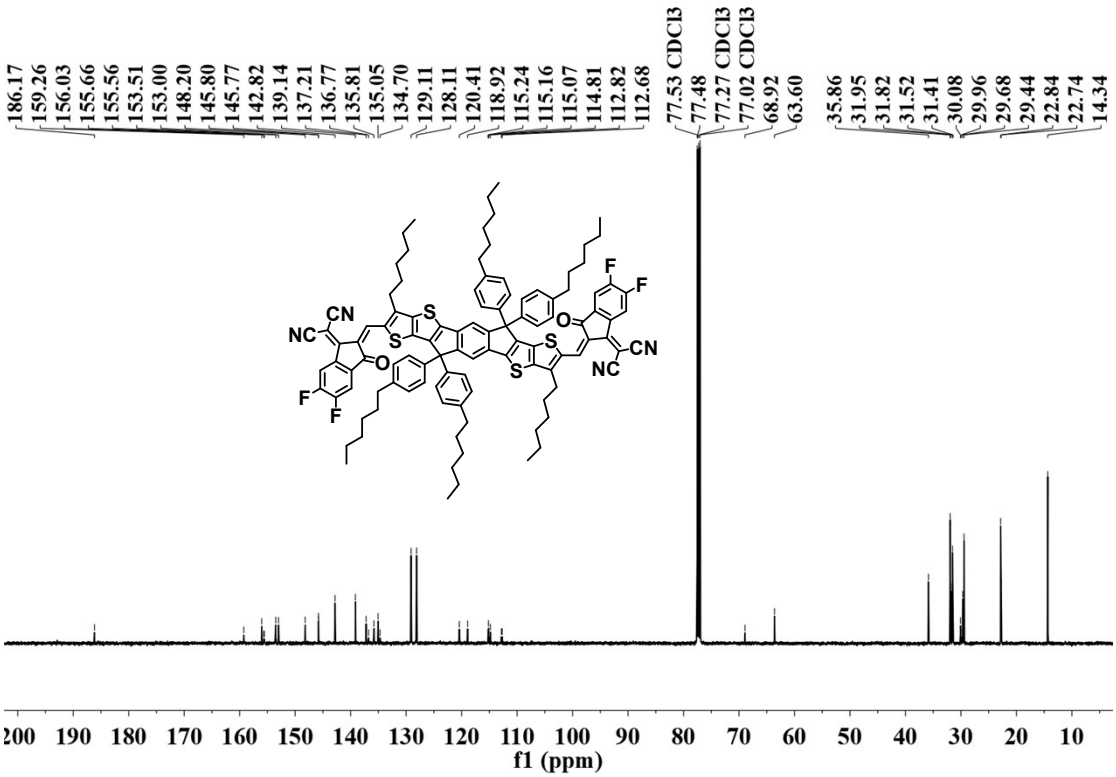

Fig. S2 ^{13}C NMR of **ITC6-4F.**

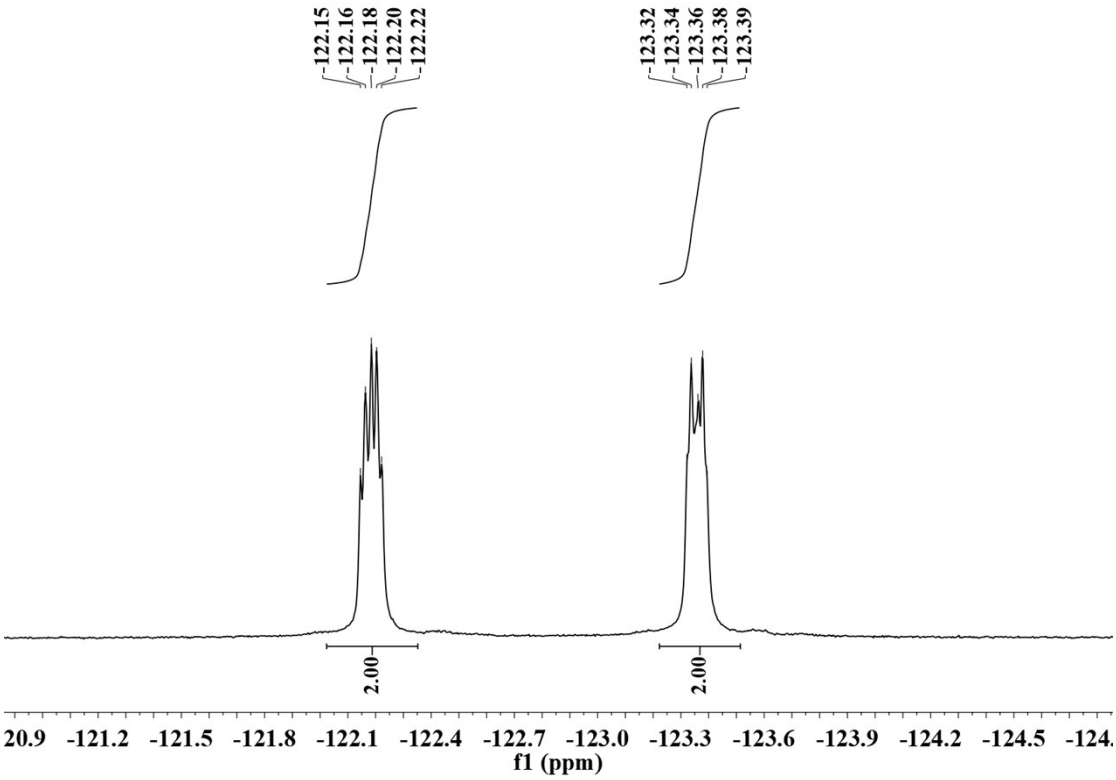

Fig. S3 ^{19}F NMR of **ITC6-4F.**

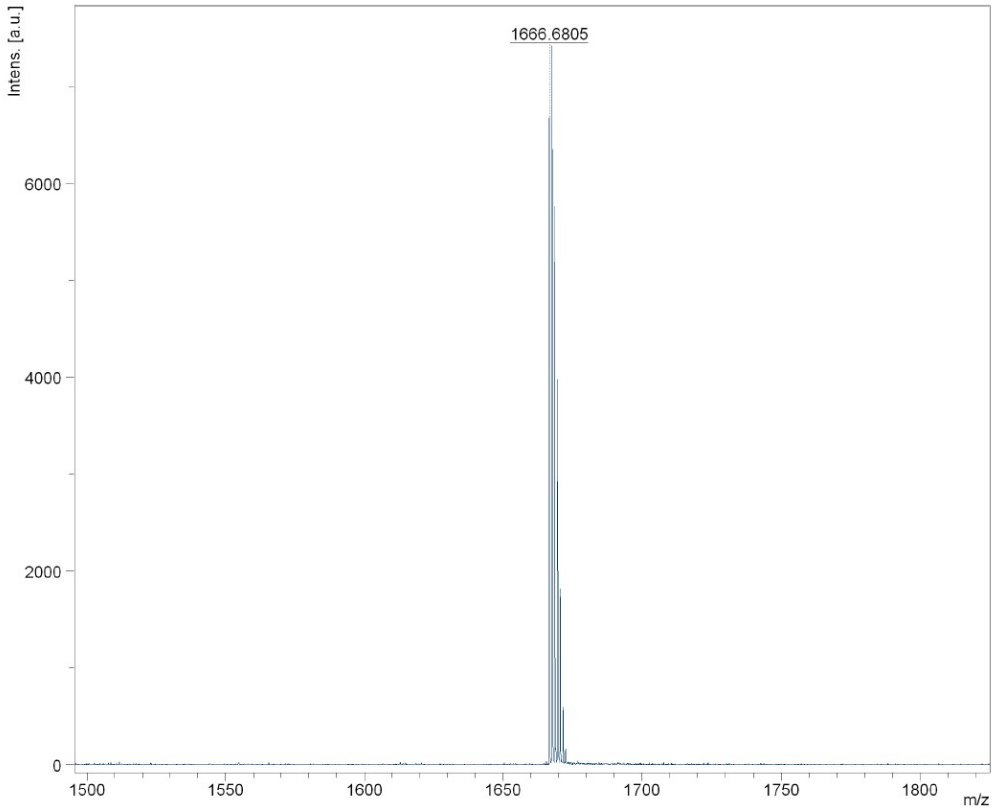

Fig. S4 Mass spectra of **ITC6-4F.**

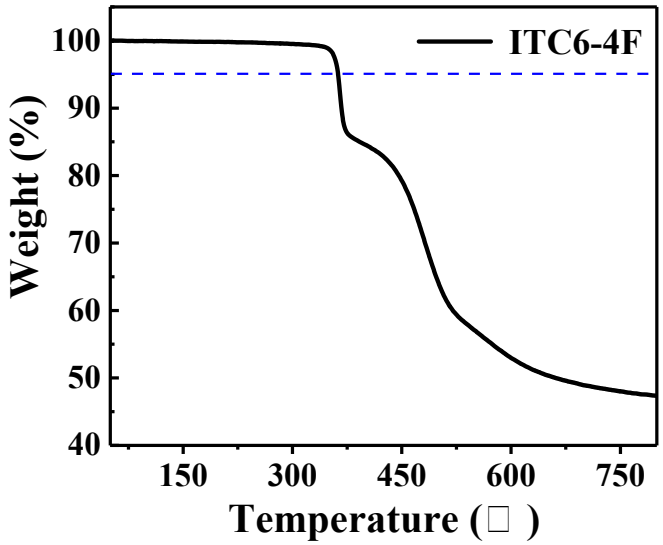

Fig. S5 TGA curve of **ITC6-4F**.

4. GIWAX patterns of neat films

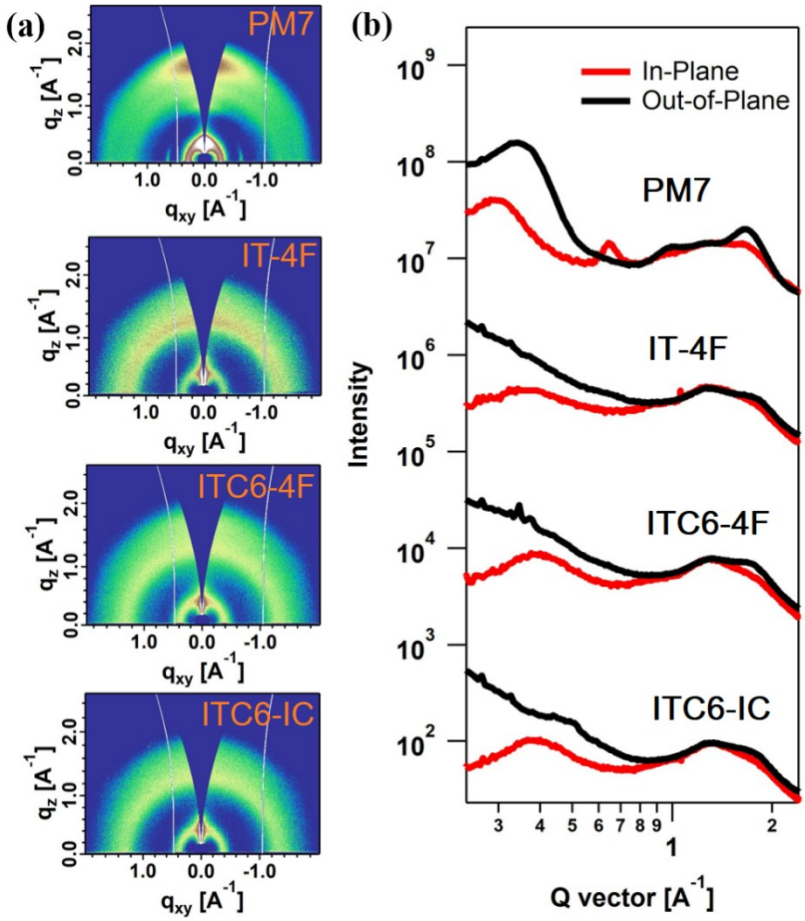

Fig. S6 a) GIWAX patterns of PM7, IT-4F, ITC6-4F, and ITC6-IC neat films; b) the related in-plane (red lines) and out-of-plane (black lines) line cuts.

5. CV measurement

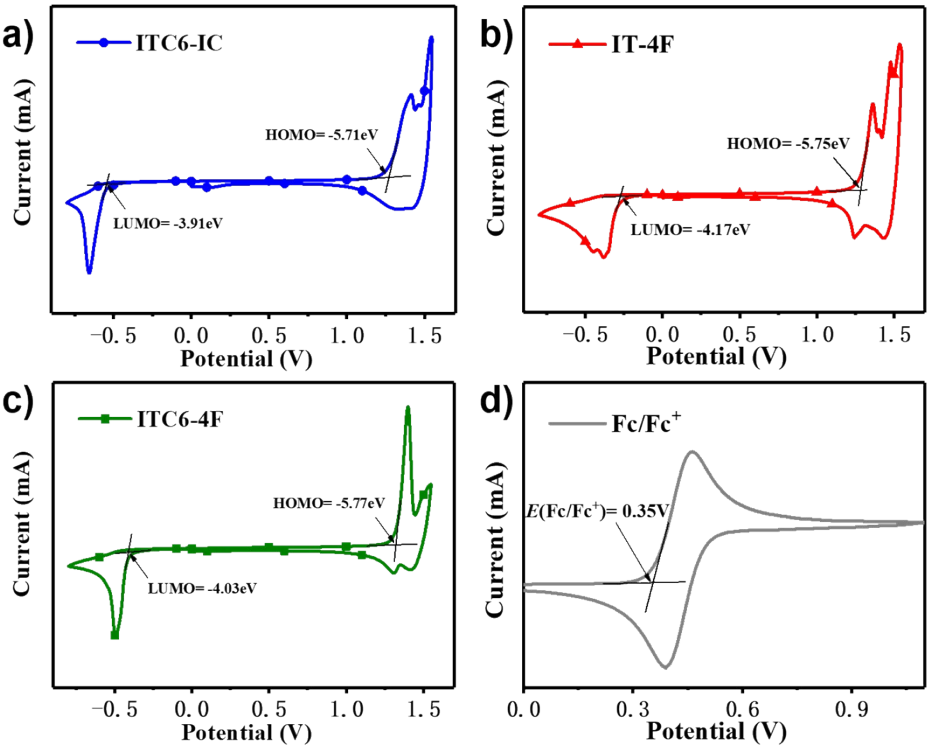

Fig. S7 CV curve of ITC6-IC, IT-4F, ITC6-4F, and ferrocene/ferrocenium

6. Fabrication and characterizations of devices.

ITO-coated glass substrates (sheet resistance = 15 Ω/square) were cleaned via sequential sonication in detergent, deionized water, acetone and isopropanol. All pre-cleaned ITO substrates were treated by oxygen plasma for 90 seconds to improve its work function and clearance. The procedure for fabricating inverted OSCs of ITO/ZnO/PM7:ITC6-4F/MoO_3/Ag is as follows. ZnO layer (ca. 30 nm) was spin-coated at a speed of 4000 rpm onto the ITO glass from ZnO precursor solution, and annealed at 200 ℃ for 30min. Then the mixture (10 mg mL^{-1} for polymer) in chlorobenzene were spin-coated on the ZnO layer to form a photosensitive layer (~100 nm). The MoO_3 (8nm) and Ag (100 nm) layer were successively deposited by thermal evaporation. The active area of the device was 3.97 mm^2.

The current density-voltage (*J-V*) curves of all devices were measured by a Keithley 2400 unit in high-purity nitrogen-filled glovebox. The AM 1.5G irradiation was

provided by a Newport solar simulator with light intensity of 100 mW cm^{-2} which is calibrated using a standard single crystal Si photovoltaic cell. The external quantum efficiency (EQE) spectra of inverted devices were obtained using a Solar Cell Spectral Response Measurement System QE-R3011 (Enlitech Co., Ltd.). The light intensity at each wavelength was also calibrated using a standard single crystal Si photovoltaic cell. The film thicknesses were measured using Bruker DektakXT stylus profiling system.

SCLC Mobility Measurements: Electron-only devices with the configuration of ITO/ZnO/active layer/PDINO/Al and hole-only devices with the configuration of ITO/PEDOT:PSS/active layer/MoO_3/Ag were used to evaluate charge mobilities by SCLC model. The fabrication conditions of the active layer were the same procedure described in the above experimental section. The charge mobilities were determined by fitting the dark current according to the following equation:

$$J = \frac{9}{8}\varepsilon_r\varepsilon_0\mu\frac{V^2}{L^3} \quad (1)$$

Where J is the dark current density (mA cm^{-2}), $?_r$ is the permittivity of free space, $?_0$ is the dielectric constant of the blend material, V is the effective voltage and L is the thickness of the active layer.

7. Theoretical calculations on ITC6-IC, IT-4F and ITC6-4F

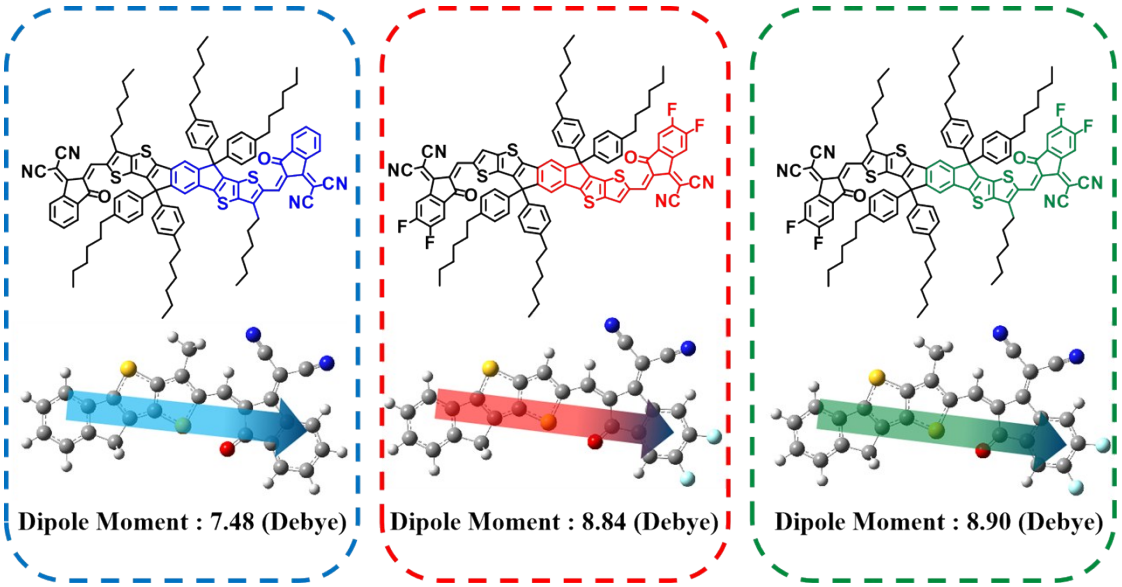

Fig. S8 DFT-based theoretical calculations on dipole moment based on simplified configurations of ITC6-IC, IT-4F, and ITC6-4F, respectively.

8. Device data

Table S1. The optimized photovoltaic parameters of devices based on PM7:ITC6-4F with different D/A ratios.

D/A	V_{OC} [a)] [V]	J_{SC} [a)] [mA cm^{-2}]	FF [a)] [%]	PCE [a)] [%]
1:0.8	0.980 (0.978±0.002)	18.65 (18.36±0.33)	63.34 (62.53±0.57)	11.58 (11.23±0.30)
1:1	0.960 (0.959±0.001)	18.94 (18.82±0.08)	64.13 (63.62±0.39)	11.66 (11.48±0.13)
1:1.25	**0.960 (0.959±0.001)**	**19.70 (19.38±0.35)**	**63.97 (63.04±0.66)**	**12.10 (11.71±0.32)**
1:1.5	0.939 (0.939±0.01)	19.38 (19.36±0.09)	62.30 (62.08±0.16)	11.34 (11.28±0.05)

[a)]The highest values and the average values in brackets were obtained from 12 devices.

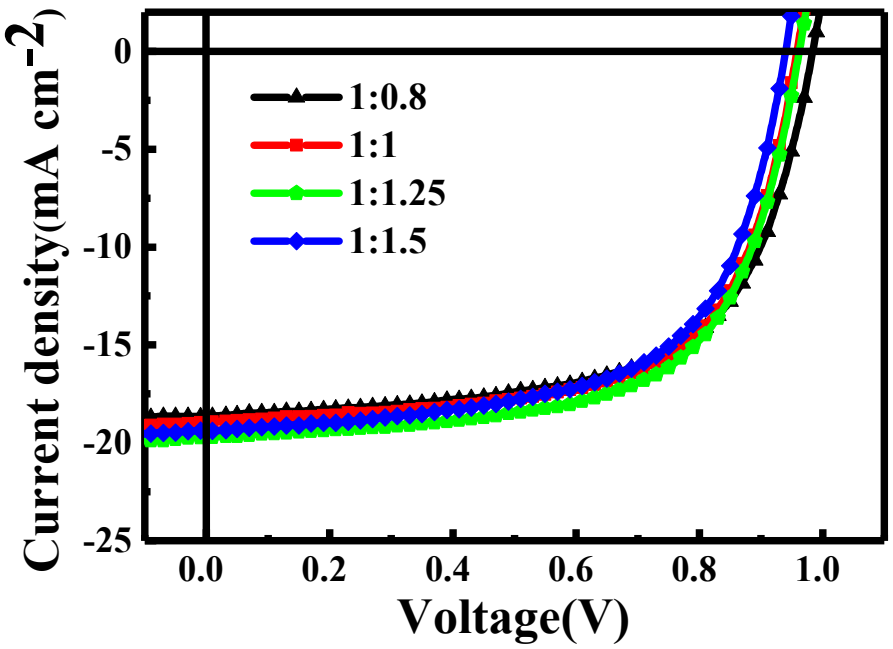

Fig. S9 *J*−*V* curves of PM7/ITC6-4F based devices with different D/A ratios.

Table S2. The optimized photovoltaic parameters of devices based on PM7:ITC6-4F (1:1.25) with different additives and volume ratios.

Additives	V_{OC} [a)] [V]	J_{SC} [a)] [mA cm^{-2}]	FF [a)] [%]	PCE [a)] [%]
0.5% DIO	0.910 (0.909±0.001)	20.79 (20.46±0.27	68.15 (67.50±0.48)	12.89 (12.55±0.27)
1% DIO	0.910 (0.908±0.002)	20.59 (20.16±0.31)	70.51 (69.90±0.61)	13.21 (12.79±0.30)
0.5%CN	0.900 (0.899±0.001)	20.92 (20.63±0.36)	68.10 (68.25±0.65)	12.82 (12.65±0.14)
1%CN	0.910 (0.909±0.01)	20.42 (20.13±0.23)	69.72 (69.51±0.52)	12.96 (12.72±0.17)
0.25%DIO+0.25%CN	**0.930 (0.928±0.002)**	**20.87 (20.52±0.300)**	**70.87 (70.19±0.75)**	**13.76 (13.37±0.27)**
0.5%DIO+0.5%CN	0.880 (0.879±0.001)	20.91 (20.53±0.32)	68.49 (67.87±0.55)	12.60 (12.25±0.30)

a) The values in parentheses are the highest values and the average values in brackets were obtained from 12 devices.

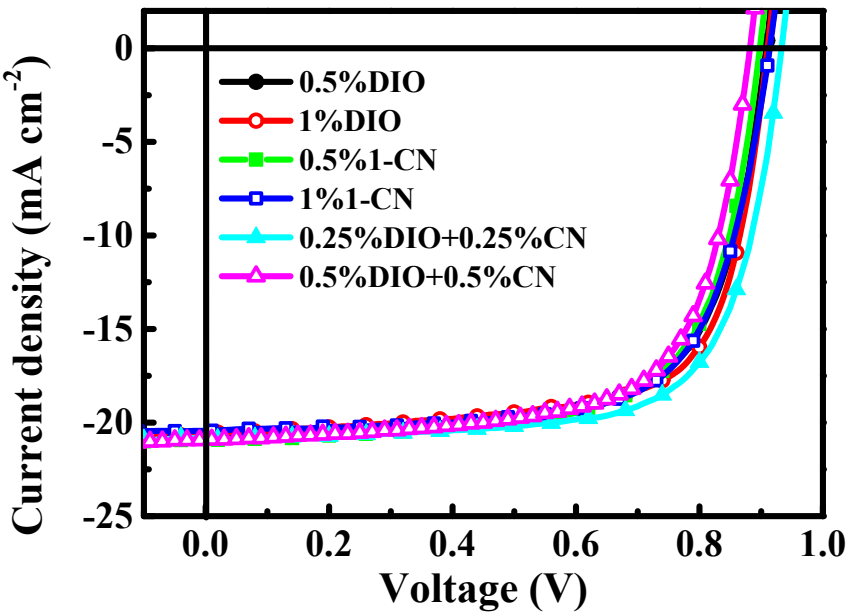

Fig. S10 *J*−*V* curves of PM7/ITC6-4F based devices with different additives and volume ratios.

Table S3. The optimized photovoltaic parameters of devices based on PM7/ITC6-4F at different thermal annealing temperature (TA) and time with 0.25%DIO+0.25%CN additives.

TA	Time [min]	V_{OC} [a)] [V]	J_{SC} [a)] [mA cm^{-2}]	FF [a)] [%]	PCE [a)] [%]
without	without	0.940 (0.939±0.001)	18.75 (18.60±0.41)	66.37 (65.56±0.78)	11.70 (11.46±0.23)
80℃	5	0.940 (0.939±0.001)	18.99 (18.86±0.12)	69.73 (69.35±0.21)	12.44 (12.28±0.13)
80℃	10	0.930 (0.928±0.002)	19.35 (19.10±0.19)	69.78 (69.46±0.81)	12.56 (12.31±0.19)
100℃	5	0.930 (0.928±0.001)	20.32 (20.13±0.11)	68.95 (68.16±0.63)	13.03 (12.73±0.27)
100℃	10	0.930 (0.928±0.001)	20.65 (20.23±0.31)	68.19 (67.43±0.70)	13.10 (12.66±0.34)
125℃	5	0.930 (0.929±0.001)	20.61 (20.34±0.15)	70.87 (70.65±0.14)	13.58 (13.35±0.20)
125℃	10	0.930 (0.929±0.001)	20.84 (20.56±0.25)	68.96 (68.68±0.44)	13.37 (13.12±0.18)
135℃	5	0.930 (0.929±0.001)	20.37 (20.14±0.18)	70.99 (70.21±0.51)	13.44 (13.14±0.17)
135℃	10	0.920 (0.918±0.002)	21.06 (19.90±0.12)	71.14 (71.01±0.51)	13.78 (12.98±0.18)
150℃	**5**	**0.900 (0.898±0.004)**	**21.64 (21.87±0.15)**	**74.31 (72.92±0.82)**	**14.47 (14.32±0.10)**
150℃	10	0.810 (0.808±0.002)	20.69 (20.62±0.15)	64.72 (63.95±0.78)	10.85 (10.65±0.22)
175℃	5	0.800 (0.798±0.003)	21.29 (21.01±0.19)	63.34 (63.12±0.20)	10.78 (10.58±0.15)
175℃	10	0.780 (0.778±0.002)	20.94 (20.67±0.22)	45.99 (45.11±0.48)	7.51 (7.25±0.24)

[a)]The values in parentheses are the highest values and the average values obtained from 12 devices.

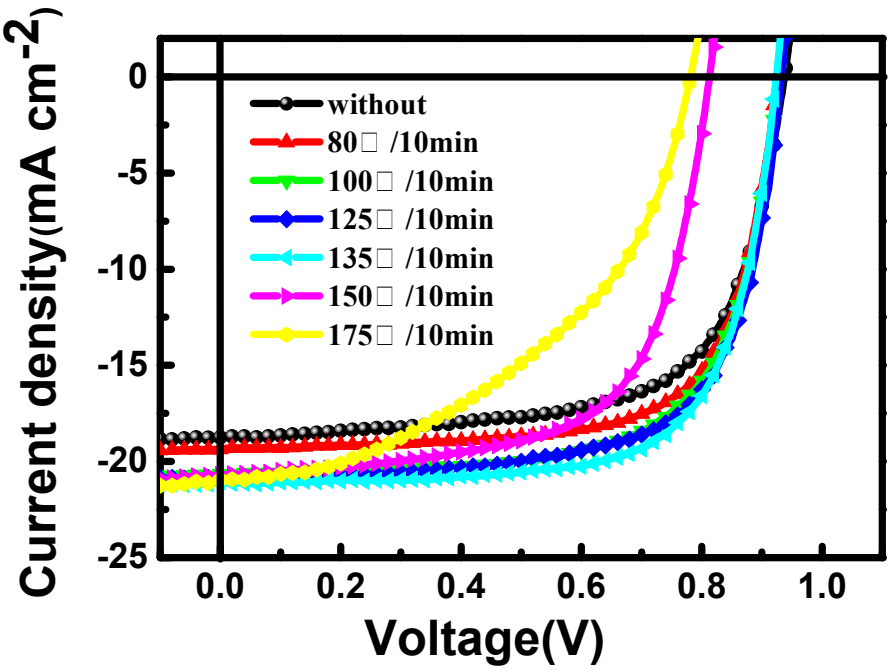

Fig. S11 *J*−*V* curves of PM7/ITC6-4F with different thermal annealing temperature for 10 min.

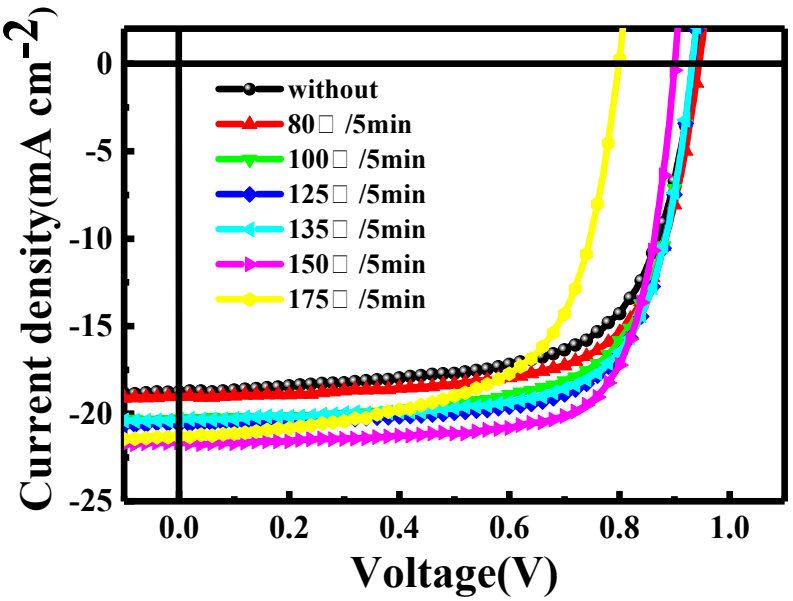

Fig. S12 *J*−*V* curves of PM7/ITC6-4F with different thermal annealing temperature for 5 min.

Table S4. Hole and electron mobilities of the neat and blend films.

Film	μ_h [cm^2 V^{-1} s^{-1}]	μ_e [cm^2 V^{-1} s^{-1}]	μ_h/μ_e
ITC6-4F[a)]	-	4.27×10^{-4}	-
IT-4F[a)]	-	3.52×10^{-4}	-
ITC6-IC[a)]	-	1.27×10^{-4}	-
PM7:ITC6-4F [b)]	4.53×10^{-4}	2.51×10^{-4}	1.80
PM7:ITC6-4F [c)]	5.67×10^{-4}	5.02×10^{-4}	1.13
PM7:IT-4F[c)]	4.34×10^{-4}	3.11×10^{-4}	1.39
PM7:ITC6-IC[c)]	2.43×10^{-4}	9.89×10^{-5}	2.46

[a)] Neat film; [b)] as-cast film; [c)] optimized film.

9. Resonant soft X-ray scattering

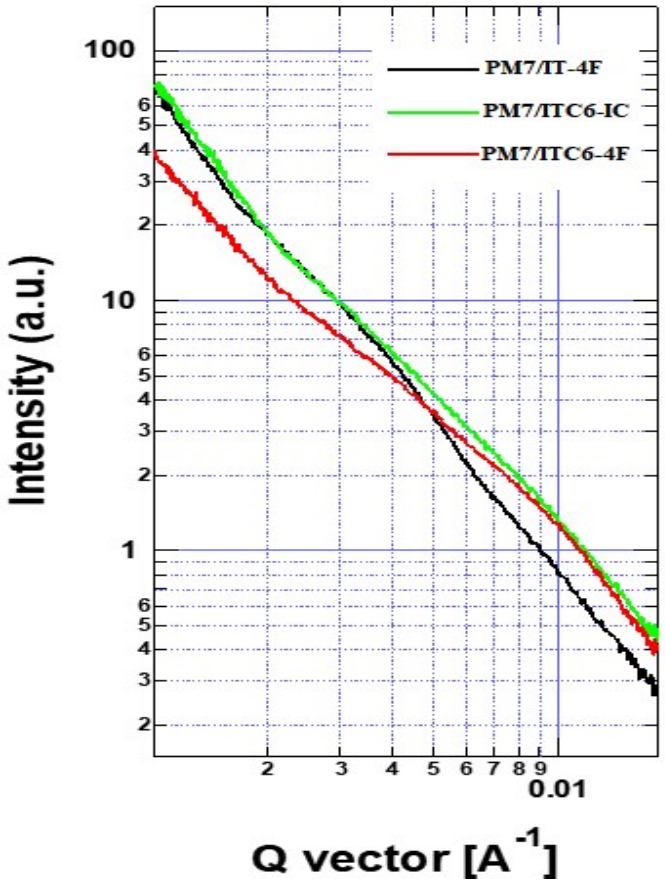

Fig. S13 RSoXS profiles of the blend films.

References

1 Z. Zhang, J. Yu, X. Yin, Z. Hu, Y. Jiang, J. Sun, J. Zhou, F. Zhang, T. Russell, F. Liu and W. Tang, *Adv. Funct. Mater.,* 2018, **28**, 1705095.